Indian Journal of Chemical Technology
Vol. 31, January 2024, pp. 44-56
DOI: 10.56042/ijct.v31i1.4596

Graphene oxide-enhanced aerosol forming composites: A study for fire extinguishing applications

Meenakshi Rohilla[1,2], Amit Saxena[1]*, Prem chand[1], Braham Prakash[1,2], Kavita Devi[1], Rajesh Kumar Tanwar[1], Rajiv Narang[1] & Yogesh Kumar Tyagi[2]*

[1]Centre for Fire, Explosive and Environment Safety, Timarpur, Delhi-110054, India

[2]Guru Gobind Singh Indraprastha University, Delhi, India

*E-mail: amitsaxena.cfees@gov.in (AS); drytyagi@gmail.com (YKT)

Received 4 August 2023; accepted 22 November 2023

Condensed aerosol-based fire extinguishing system (CAFES) has emerged as the most proficient fire extinguishing system since the implementation of Montreal protocol 1987. Aerosol forming composite (AFC) is the key constituent of CAFES. For the first time, graphene oxide-based AFCs have been prepared and characterized for use in extinguishing fires. Catalytic activity of bulk graphite, graphite oxide & graphene oxide (1, 3 & 5 %, w/w) on combustion characteristics of AFC is examined by incorporating them in the base AFC. Graphene additives are synthesized and characterized using instrumental techniques such as XRD, FTIR, Raman, SEM and TEM. AFCs with catalysts are also assessed for performance using parameters such as combustion efficiency, minimum fire extinguishing concentration (MEC), burn rate, combustion temperatures and activation energies. Maximum reduction in combustion temperature from 455 to 409 ℃ is observed with 5% graphene oxide containing AFC. Addition of 1% graphene oxide to base AFC remarkably has augmented the performance of AFC by enhancing the burn rate by 12.89%. Prepared high burn rate AFC is under further investigations for potential use in cutting-edge aerosol-based firefighting systems.

Keywords: Aerosol forming compositions, Burn rate, Combustion, Fire extinguishment, Graphene oxide

Introduction

Halon 1301 had been regularly used as the most proficient fire extinguishing agent since 1940s due to its low cost and high efficiency. But it was banned in 1987 by Montreal Protocol due to ozone depletion potential[1]. Since then, researchers from all over the world worked for the development of Halon alternatives. Many halon alternatives were developed such as water mist[2], dry powders[3], inert gases[4], carbon dioxide[5], hydroflouro carbons[6], aerosols [7] etc. Among these, condensed aerosol-based fire extinguishing system (CAFES) evolved as the most promising halon alternatives due to zero ozone depletion potential and high effectiveness. It also has negligible global warming potential and atmospheric lifetime. Other halon alternatives such as inert gases, hydrofloro carbons, carbon dioxide did not establish as good Halon alternative due to the requirement of pressurized cylinders, large spaces, high installation & maintenance cost etc. On the other hand, CAFES entail; no hefty pipelines & pressurized cylinders, low installation & maintenance cost, compact, environmentally friendly, high shelf life.

A pyrotechnic aerosol forming composite (AFC) composition basically includes an oxidizer, fuel, binder, and technological catalysts. Pyrotechnically generated aerosols are produced from the combustion of organic fuel cum binder with inorganic oxidizers and salts. Oxidizers provide the required oxygen and fuel takes up that oxygen to complete the combustion rection. The role of binder is to hold together all the solid ingredients and provide the sufficient strength to the composite[8]. Several technological catalysts are generally added in the AFC for various purposes. Majorly potassium nitrate is used as an oxidizer due to its superior fire extinguishing activity (due to potassium radical) and phenol formaldehyde resin as fuel cum combustible binder. On combustion of AFC within CAFES, superfine particles mostly comprised of carbonates, bicarbonates; and inert gases such as carbon dioxide, nitrogen & water vapour are generated. These aerosol particles quench the fire supporting radicals (O•, H• & OH•) by recombination reactions, and inert gases extinguish fire by physical mechanism[9]. CAFES shows versatile applications in numerous places such as energy storage systems, transportation,

storage rooms, power generation, heavy industries, commercial marines, defence platforms etc.[10].

In recent times, graphene oxide has indicated promising results in various fields such as electrochemistry, solar cells, catalysis, electronics, composites, etc.[11-15]. It gained a lot of attention due to its high thermal conductivity, high mechanical strength, light weight, and large surface area. More recently, an interest has been developed in researchers towards its catalytic behaviour in energetic applications due to its high thermal conductivity, radiant heat transfer and high heat of combustion[16]. Li et al.[17] introduced graphene oxide to HMX for enhancing the safety measures of HMX. Graphene oxide in combination with metal/metal oxide has been incorporated in propellants for decomposition studies. Yan et al.[18] investigated the catalytic effect of ferric oxide/graphene oxide on the thermal decomposition of ammonium perchlorate. An et al.[19] prepared Cu_2O-PbO/GO and CuO-PbO/GO nanocomposites for enhancing the burn rate of double base propellants. Zhang et al.[20] employed nitrated graphene oxide as an energetic burn rate catalyst to study its impact on the decomposition of ammonium perchlorate. A lot of studies have been performed showing the catalytic behaviour of graphene oxide with metal & metal oxides on thermal decomposition of ammonium perchlorate, solid rocket propellant, explosives etc.

Fire extinguishing efficiency of AFC mainly depends on its burn rate and combustion temperature. Therefore, the addition of graphene oxide may affect the burn rate and combustion temperature of AFC due to its superior heat transfer and thermal conductivity. Till date, no study has been reported to showcase the effect of different graphitic forms on combustion pattern of AFCs. Therefore, for the first time, graphene oxide based AFCs have been prepared and characterized. Also, a comparison between bulk graphite, graphite oxide and exfoliated graphene oxide based AFCs with loading rate of 1, 3, and 5 % has been made. Catalytic activity has been determined by studying various performance parameters. These studies have been performed with a goal to develop highly efficient AFCs for use within fast fire extinguishing CAFES.

Experimental Section

Materials

Potassium nitrate, potassium permanganate, graphite powder, conc. sulphuric acid and conc. nitric acid of reagent grade were purchased from M/s CDH fine chemicals Ltd, India. Phenol formaldehyde resin (grade-ARP7911) was purchased from M/s Apex plastics Pvt. Ltd., Delhi. All chemicals were used without further purification. Double distilled water was used for all preparations.

Synthesis of graphene oxide

Graphite oxide was synthesized using Hummers' method with some modifications. In modified Hummer's method, alternative quenching agents have been explored, and nitric acid (HNO_3) has been used. HNO_3 can neutralize excess permanganate ions and contribute to adjusting the pH, similar to hydrogen peroxide. The addition of HNO_3 is a part of the protocol to stop the oxidation process and adjust the pH of the reaction mixture.

Graphite powder (12 g) was taken in 2 L round bottom flask. Sulphuric acid (500 mL) and HNO_3 (50 mL) was added with continuous stirring in an ice bath. The temperature of the solution was maintained at below 5°C using ice bath. Potassium permanganate ($KMnO_4$) (36 g) was added gradually maintaining the temperature of solution below 5°C only. After complete addition of $KMnO_4$, ice bath was removed, and the solution was stirred for 24 h at room temperature. Then, distilled water (260 mL) was added to the mixture and the temperature of the solution was maintained below 80°C with continuous stirring for 30 min. Afterwards, 900 mL distilled water was added to the mixture and decanted. 400 mL 20% HNO_3 was added and heated to 80°C for 2 h. The resulting suspension was washed and centrifuged at 9000 rpm repeatedly till the pH of the solution reached 6-7. Thereupon, the obtained product was dried in an oven at 60°C for 6-7 h. The synthesized graphite oxide was exfoliated to graphene oxide nanosheets by thermal exfoliation at 300°C under atmospheric pressure. The synthesis procedure is depicted in Fig. 1.

Preparation of aerosol forming composites incorporating bulk graphite, graphite oxide and graphene oxide

Fig. 2 depicts the schematic for the preparation of AFC with and without catalysts. Potassium nitrate (80%) was dried in oven and sieved through 75 µm sieve. Then, graphene oxide (1, 3 & 5%, w/w) was combined with potassium nitrate using a ball mill to obtain a solid mixture. Afterwards, phenol formaldehyde resin solution was prepared with acetone as a solvent and added continuously to the above solid mixture with constant stirring (40°C) to

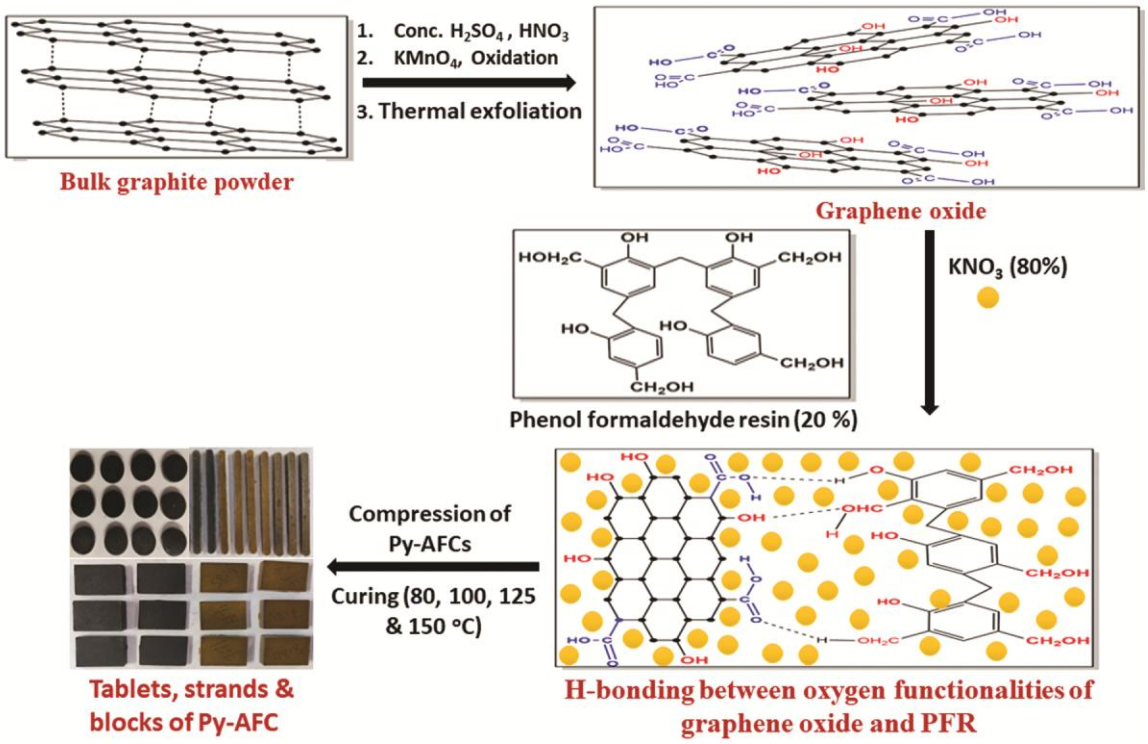

Fig. 1 — Schematic representation of preparation of AFCs

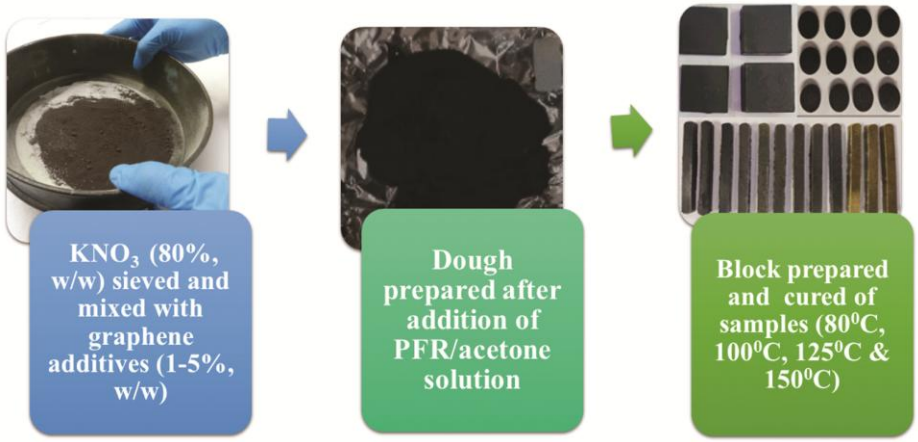

Fig. 2 — Schematic of preparation of AFC incorporating graphene oxide

prepare a dough. The dough was then dried, grounded, and compressed using hydraulic press in the form of a tablet (11 mm diameter, 1 g), a cuboid strand (100 x 6 x 6 mm, 8 g) and a cuboid block (25 x 25 mm) applying 165 MPa pressure for 5 min. Prepared AFCs were then cured at different temperatures (80, 100, 125 and 150 °C) for 4 h at each temperature. AFCs incorporating bulk graphite and graphite oxide were also prepared by replacing graphene oxide in above procedure by them.

Characterization of catalysts and AFCs incorporating catalyst

Characterization of synthesised catalysts

X-ray diffraction pattern of synthesized catalysts and produced aerosols was recorded at Bruker D8 advance X-ray diffractometer. CuKα radiation (λ = 1.5405 Å) was used as a source with a measurement angle of 2θ (5-80°, scan rate 5 °/min). Recorded patterns were compared with JCPDS. For identifying the chemical bonding in graphene and aerosols, FTIR spectra was recorded at Thermo-fisher

FTIR (NICOLET 8700, Waltham, Massachusetts). The microstructure, size and morphology of catalysts were determined by scanning electron microscope (SEM) (Zeiss Cambridge, UK EVO, MA15) and transmission electron microscope (TEM) (Jeol JEF-200 Japan).

Characterization of AFCs incorporating synthesised catalysts

Thermo-kinetic properties (combustion temperature, activation energy) of AFC with and without catalysts were studied using simultaneous thermogravimetric analyser generated differential scanning calorimeter (TGA-DSC), Perkin Elmer diamond Singapore. Cured and grounded AFC samples (5 mg) were analysed at 10 ℃/min heating rate under N_2 atmosphere from 50 to 500 ℃ using alumina as reference.

Combustion efficiency is the percentage of aerosol generated after combustion of AFC. The test was performed by the method used in our previous work[21]. For performing the test, AFC tablets were prepared and were placed at the centre of the pre-weighed glass Petri dish and then ignited using nichrome wire, as shown in Fig 3a. After combustion, the petri dish was weighed again. Amount of aerosol formed (combustion efficiency) was then calculated by subtracting the percentage residue formed from 100.

Burn rate is an important factor, which determines the combustion behaviour of AFCs. The burn rate was calculated according to equation, B.R. = L/t, where 'L' is the length of the AFC strand and 't' is the time of burning. For performing burn rate measurements, AFC strands (100 mm x 6 mm x 6 mm) were burnt from one end to another using nichrome wire. Time of burning was observed using stopwatch and video camera as shown in Fig 3b. For establishing the reproducibility of the results, tests were performed in triplicates. Combustion efficiency (percentage of aerosol generated after combustion of AFC) was determined by burning 1.0 g tablet of AFC in stainless steel dish[21].

Fire extinguishing efficacy of AFCs was studied by investigating its minimum fire extinguishing concentration (MEC), i.e., the minimum amount of sample required to extinguish the fire in unit volume[22]. It is calculated in g/m^3. Cuboidal blocks with a dimension of 25 x 25 mm were made for this experiment. All tests were carried out in a mild steel fire test chamber that had the following measurements: 48.5 x 49 x 48.3 cm, 0.104 m^3 volume. An observation window measuring 10 cm x 10 cm was placed in front to record the class B fire extinguishment test (Fig. 4). A stainless-steel fuel pan with dimensions of 5 cm in height and 9.8 cm in diameter was placed in the centre of the chamber and used to create a 33 kW n-heptane smallpool fire. In the centre of the chamber, a platform measuring 5 cm high held the variable number of cuboidal AFC blocks. Both the fuel pan and the AFC blocks were connected to nichrome wire with 24 V power source to enable their activation. Prior to the tests, an n-heptane pool fire was self-extinguished in a sealed chamber. It was found that the fire had extinguished itself in 65 seconds. Then, for the tests, first, the fuel was ignited using nichrome wire and then after 30 s of pre burn time[23], AFC was ignited. Fire extinguishing time was recorded using stopwatch and camera. MEC was calculated at four fire extinguishment times, i.e., 5, 10, 20 and 30 s for better understanding the fire extinguishing efficiency of AFCs.

Solid particulates of aerosols as well as gaseous products are formed on combustion of AFCs. These solid aerosol particles are mainly responsible for

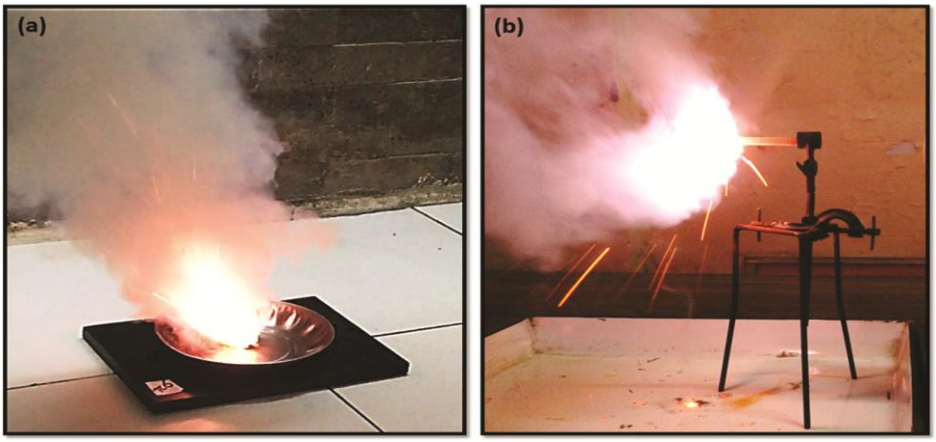

Fig. 3 — Laboratory methods for performing (a) combustion efficiency measurement and (b) burn rate tests

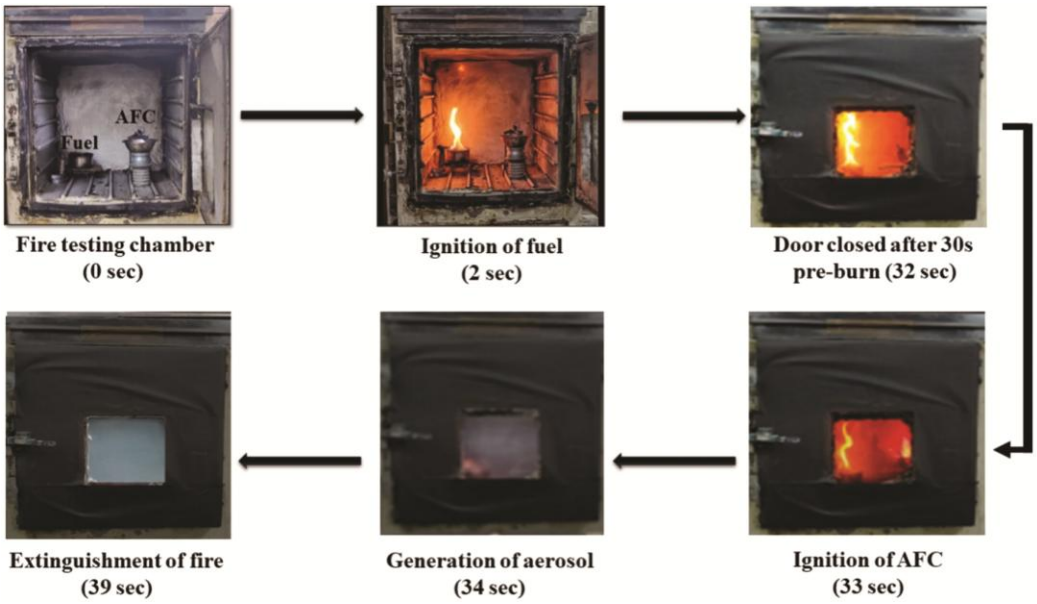

Fig. 4 — Schematic of test for determining minimum fire extinguishing concentration of AFCs

quenching the fire propagating radicals. Therefore, for investigating composition and structure of solid aerosols, these were collected on glass plate. For collection, glass plate and AFC were kept inside the chamber. Thereafter, AFC ignited, and the chamber door remained closed for 1 h for settlement of aerosol particle on glass plate.

Result and Discussions

Characterization of synthesized catalyst

FTIR spectra for graphite oxide (Fig 5a) was recorded and the functional groups identified in sample were O-H stretching vibrations at 3400 cm^{-1}, C=O stretching of COOH groups at 1724 cm^{-1}. Stretching of the sp^2-hybridized C=C bond at 1622 cm^{-1}. Two peaks at 1347 and 1047 cm^{-1} were attributed to the stretching vibrations of carboxyl C=O, epoxy-alkoxy C–O groups, respectively[24]. FTIR spectrum of exfoliated graphene oxide was also recorded. In this spectrum, the C=O stretching of COOH groups was observed at 1732 cm^{-1}. The stretching of the aromatic hybridized C=C bond appeared at 1561 cm^{-1}. The peak at 1132 cm^{-1} was attributed to the stretching vibrations of epoxy C–O. In graphene oxide the peak due to O-H stretching vibrations at 3400 cm^{-1} was completely disappeared. There was no peak corresponding to oxygen functionalities in the spectra of graphite powder as no functional group is present in it.

Graphite oxide is an oxidized form of graphite. It consists of layers of graphene sheets with oxygen-containing functional groups attached to the basal plane. Graphene oxide is a single layer of graphene with oxygen-containing functional groups, similar to graphite oxide but in a more dispersed and single-layer form. Difference in the FTIR spectra of graphite oxide and graphene oxide can be made on points such as intensities of peaks and peak broadening. A single layer of graphene oxide would have fewer oxygen-containing functional groups compared to a stacked or multilayer structure. Therefore, as can be seen in Fig. 5a, the intensities of peaks associated with oxygen-containing groups (e.g., O-H, C=O, C-O) are relatively low, it may suggest a more monolayer-like structure. A single layer of graphene oxide exhibits broader peaks compared to stacked layers due to the increased exposure of functional groups on the surface. Characteristic peaks were observed for bulk graphite, graphite oxide and graphene oxide in the X-ray diffractogram and it matches with the standard JCPDS data (file No. 33 0664). A strong peak at (002) plane centred at 10.86° is the characteristic peak of graphite oxide[25] as shown in Fig 5b. This peak shifts to 24.22° in case of graphene oxide as due to thermal exfoliation, many functional groups are lost, and graphene oxide tends acquire its original structure. A peak at 26.42° corresponds to (001) plane which is characteristic peak of graphite.

Graphite powder exhibited a characteristic XRD pattern with sharp diffraction peaks. The main diffraction peak, known as the graphite (002) peak, is typically observed at a low 2θ angle, indicating the

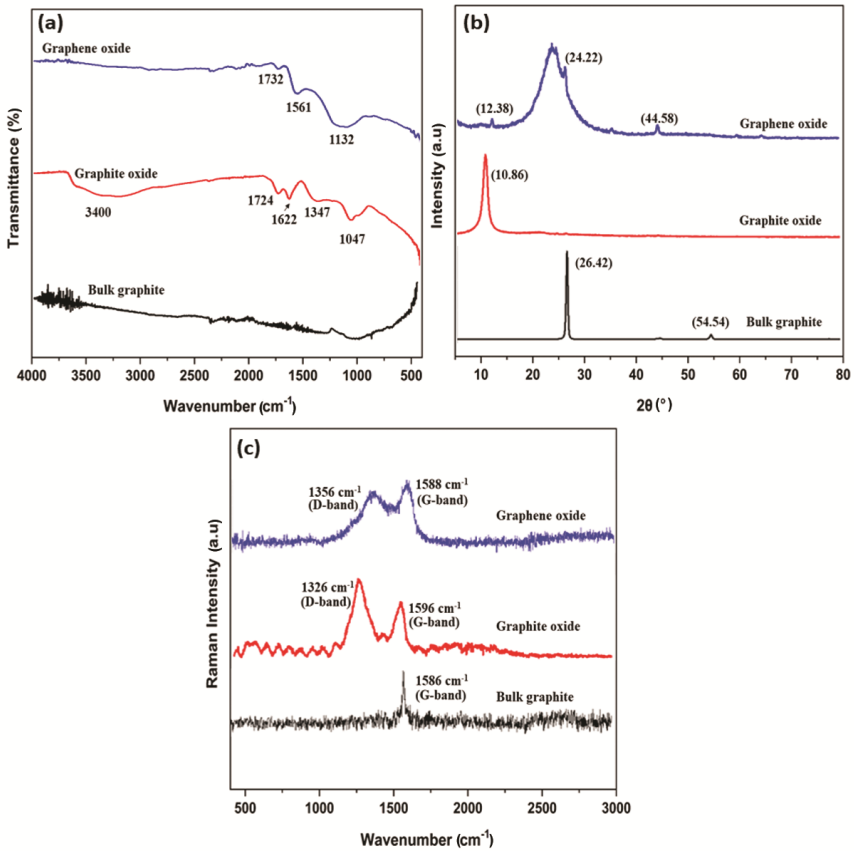

Fig 5 — Characterization of bulk graphite, graphite oxide and graphene oxide using (a) FTIR, (b) XRD and (c) Raman analysis

layered structure of graphite. The intensity of the (002) peak is relatively high, reflecting the well-ordered stacking of graphene layers in graphite. Graphite oxide, resulting from the oxidation of graphite, shows changes in the XRD pattern compared to graphite powder. The (002) peak shifted to higher 2θ angles, indicating an increase in interlayer spacing due to the introduction of oxygen-containing functional groups between the graphene layers. The broadening of the peak is also common.

Graphene oxide, which is typically a single layer or a few layers thick, showed a less defined (002) peak compared to graphite oxide. The (002) peak was observed, but it was even broader, indicating a reduced ordering in the graphene layers. The intensity of the (002) peak was lower compared to graphite powder, reflecting the reduced stacking of layers in graphene oxide.

D and G bands in the Raman spectra of graphitic structures are most prominent peaks. D band corresponds to defects and distortion in the hexagonal graphitic structure and G band corresponds to vibration of sp^2 carbon atoms due to their E_{2g} mode scattering. Two pronounced peaks can easily be seen in the Raman spectra, centered at 1351 and 1593 cm^{-1} corresponding to D and G band of graphite oxide, respectively[26] (Fig 5c). I_D/I_G ratio also tells a lot about the degree of distortion in the graphite structure. In case of bulk graphite there's no D band showing absence of any distortion but in cade pf graphite oxide D band appeared with I_D/I_G ratio of 0.93. On thermal exfoliation to obtain graphene oxide, I_D/I_G ratio decreased to 0.76 showing decrease in the degree of defect.

To investigate the size and morphology of the samples, scanning electron microscopy was performed. The SEM images of the graphite powder, as-prepared graphite oxide and exfoliated graphene oxide shown in Fig 6 a, b, and c, respectively, indicated that graphite oxide has a flack's structure, whereas graphene oxide indicated flower shape structures with clear layer separations.

When comparing graphite powder, graphite oxide, and graphene oxide using SEM, distinct differences in their surface structures can be observed. Graphite powder typically exhibits a layered structure, with

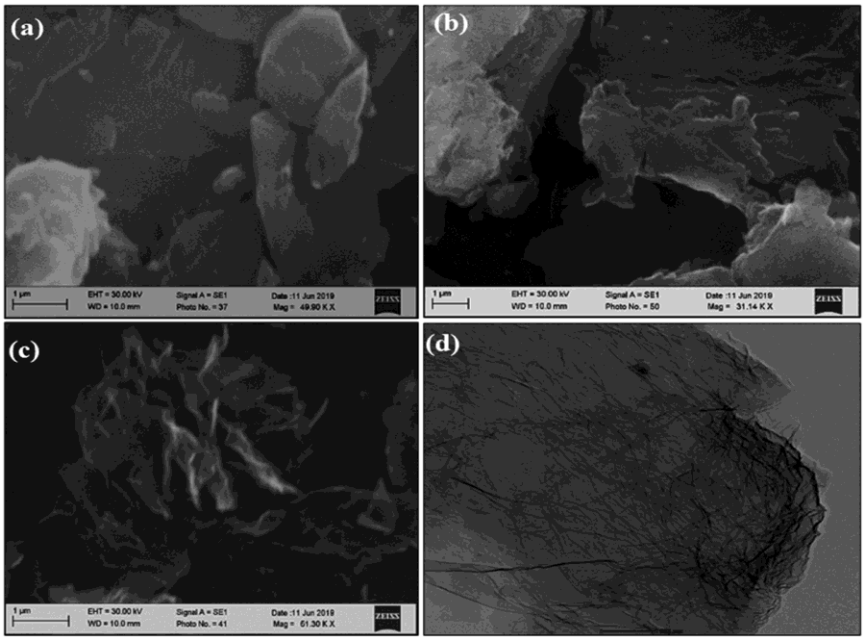

Fig. 6 — SEM images of (a) bulk graphite, (b) graphite oxide (c) graphene oxide, and (d) TEM image of graphene oxide

individual graphene layers stacked on top of each other. The surfaces of graphite particles tend to be relatively smooth due to the layered structure of graphene as can be seen in Fig. 6a.

Graphite oxide, resulting from the oxidation of graphite, often has a more irregular and rougher surface compared to graphite powder as shown in Fig. 6b.The oxidation process can lead to the separation of individual graphene layers, resulting in more dispersed and less stacked particles. SEM reveals the presence of surface features, such as wrinkles, folds, and irregularities, which are associated with the introduction of oxygen-containing functional groups during the oxidation process[27].

Graphene oxide being a form of single-layer or few-layer graphene, typically appears as individual sheets or small stacks of sheets[28]. Thinner and more transparent sheets compared to graphite oxide, the individual graphene oxide sheets appear thinner and more transparent in SEM images, (Fig. 6c). The TEM image of exfoliated graphene oxide depicts a crystalline wrinkled paper like morphology with single or a few layers (Fig. 6d). The presence of these wrinkles and folds in the exfoliated sheets of graphene oxide exhibits a characteristic feature of few layered graphene oxide.

Graphene oxide possesses oxygen-containing functional groups, such as epoxides, hydroxyls, and carboxyl, introduced during the oxidation process. These functional groups disrupt the regular hexagonal lattice structure of pristine graphene, leading to a decrease in overall crystallinity. The incorporation of oxygen-containing functional groups in graphene oxide increases the interlayer spacing between graphene sheets compared to pristine graphite or graphene. This expansion is often observable in XRD patterns as a shift and broadening of the (002) peak, indicating a reduction in the stacking order.

Characterization of performance parameters of AFCs

Thermal Analysis of AFCs

Catalytic effect of bulk graphite, graphite oxide and graphene oxide on AFCs was examined using simultaneous TGA generated DSC at a heating rate of 10 ℃/min. TGA curves indicated the combustion of AFC in the range 409-455 ℃ as shown in Fig 7. In TGA as can be seen, in case of addition of 1 & 3 % graphite powder & graphite oxide, sharp peaks are obtained. As the percentage of graphite powder is increased, curves are observed instead of sharp peaks. This is probably due to incomplete combustion (decomposition) due to pyrolysis phenomenon. Same can be seen in case of graphene oxide also, sharp dip is not obtained. In some TGA curves a sudden dip in weight loss was observed, which even led to negative values in the curve. The reason behind this may be because of the instant release of generated hot gases during combustion of AFC and disturbance of position of pan which is holding the AFC sample. Others are showing pyrolysis at higher temperatures[29].

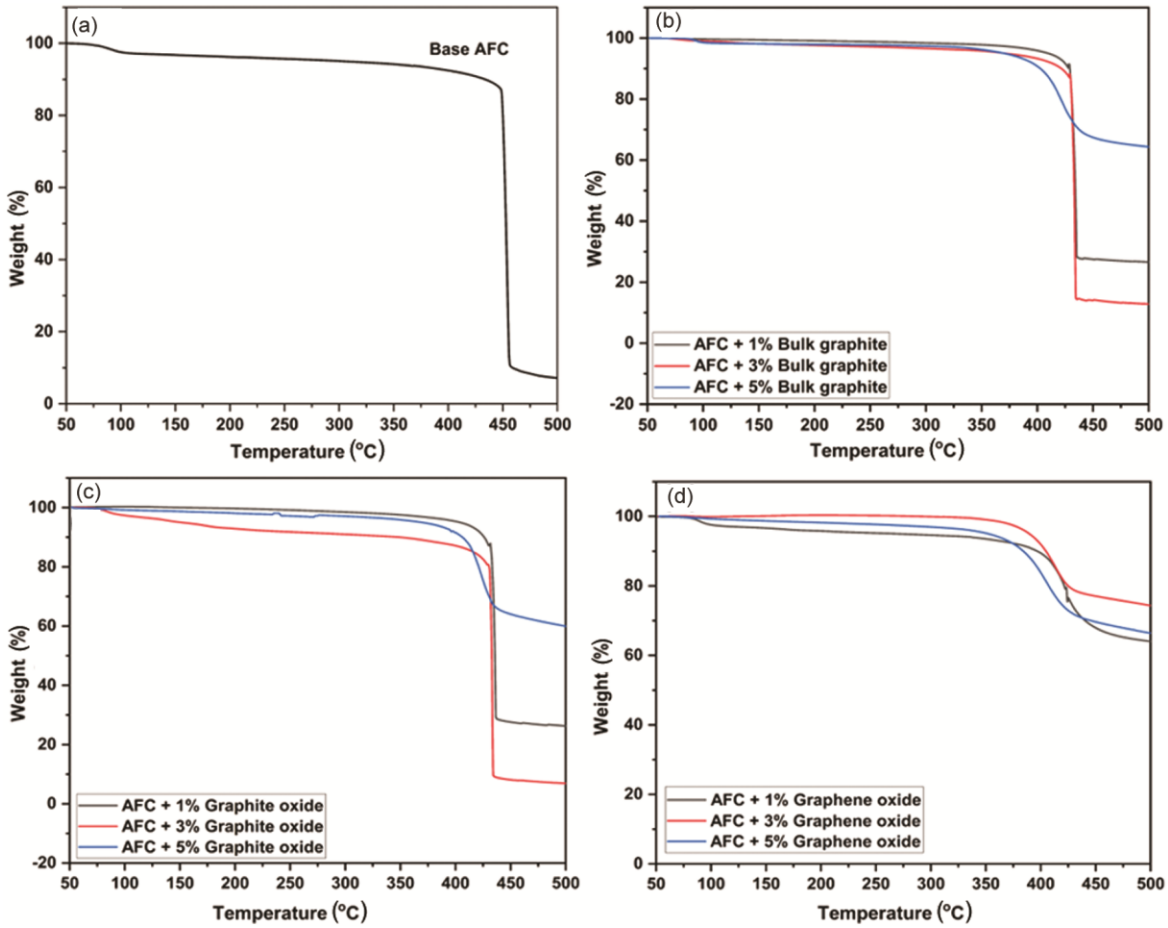

Fig. 7 — TGA curves of (a) base AFC, AFC with (b) bulk graphite, (c) graphite oxide and (d) graphene oxide (1, 3 & 5 %)

The residual masses of AFCs obtained from TGA curves on addition of graphite powder, graphite oxide and graphene oxide are (12-64 %), (7-60 %) and (64-74 %), respectively.

In the DSC curves, endothermic peak around 130 ± 5 ℃ was attributed to the crystallographic phase transition of potassium nitrate from orthorhombic to rhombohedral[30] (Fig. 8). The melting of potassium nitrate was observed as endotherm at 334 ± 5 ℃. An exothermic peak at 409-455 ℃ corresponded to the combustion of AFC. Combustion temperature decreased on increasing the percentage of catalysts. Base AFC showed the combustion temperature at 455 ℃, which reduced to 435, 434 & 430 ℃ on addition of 1, 3 & 5 % bulk graphite, respectively. Further reduction in combustion temperature of 436, 433 & 427 ℃ and 420, 417 & 409 ℃ was observed on addition 1, 3 & 5 % graphite oxide and graphene oxide, respectively. AFC with 5% graphene oxide showed the maximum reduction (10.1%) in combustion temperature.

Effect of catalyst on performance of AFCs

AFCs were also analysed for their performance parameters such as combustion efficiency, minimum fire extinguishing concentration and burn rates. In case of AFC having bulk graphite, combustion efficiency found lesser as compared to graphite oxide and graphene oxide-based samples. The presence of oxygen groups in case of graphite oxide and graphene oxide[31], facilitated the redox reaction between oxidizer and reducer (PFR). The combustion efficiency significantly surpassed the values reported in the literature, ranging from 48% to 70%, reaching an impressive 79.88% upon the incorporation of graphene oxide into the AFC[32-35]. Samples with graphite oxide or graphene oxide indicated similar combustion efficiencies. On increasing the percentage of graphite oxide or graphene oxide from 1 to 5%, combustion efficiency reduced as shown in Fig. 9a. The reduction may be due to the increase in carbon content present in the graphitic structure, which disturbed the stoichiometry of the redox ingredients.

Burn rate plays a vital role in defining the efficacy of AFC for fire extinguishment. Higher burn rate AFCs provide a directional flow of aerosols and fill the fire zone in lesser time. This facilitates the fire extinguishment in less time. When the percentage of catalysts is increased (1-5 %) in AFCs, burn rate increased, Fig 9b. AFC with 5% graphene oxide indicated the burn rate as 11.78 mm/s, whereas the base AFC indicated 9.45 mm/s. Increased burn rate with graphene oxide was due to its higher thermal conductivity. Possibly, AFC with 5% graphene oxide facilitated the energy transfer from the reacting to the pre-reacting layers of the composite[36]. In literature, burn rate of AFC with many additives and catalyst was observed to be in range of 1.5 to 7.0 mm/s [37-38]. This is much lower than the burn rate observed on addition of graphene oxide in AFC (11.78 mm/s).

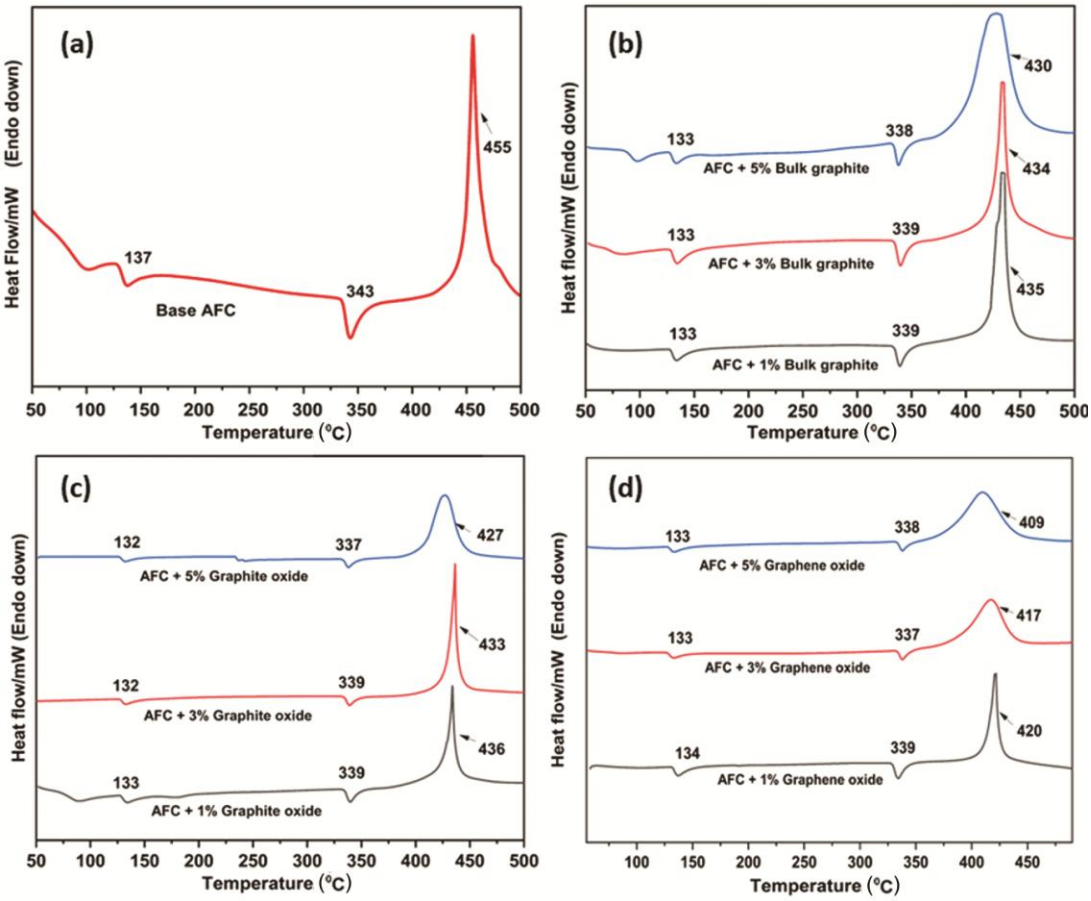

Fig. 8 — DSC curves of (a) base AFC, AFC with (b) bulk graphite, (c) graphite oxide and (d) graphene oxide (1, 3 & 5 %)

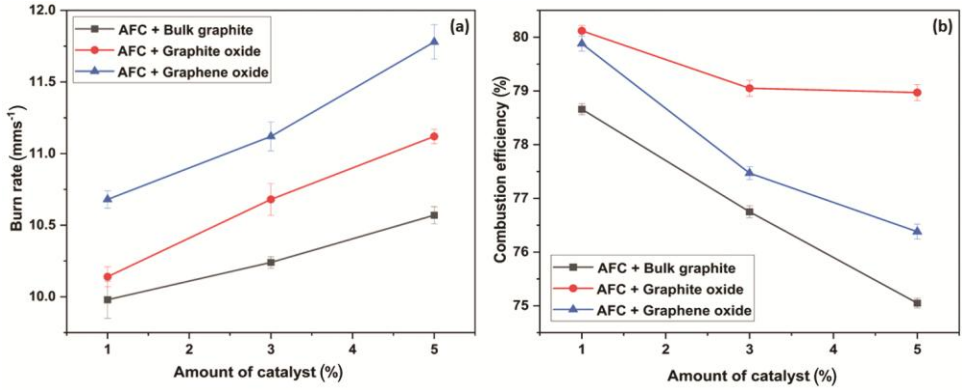

Fig. 9 — (a) Combustion efficiency and (b) burn rate of AFC with and without catalyst

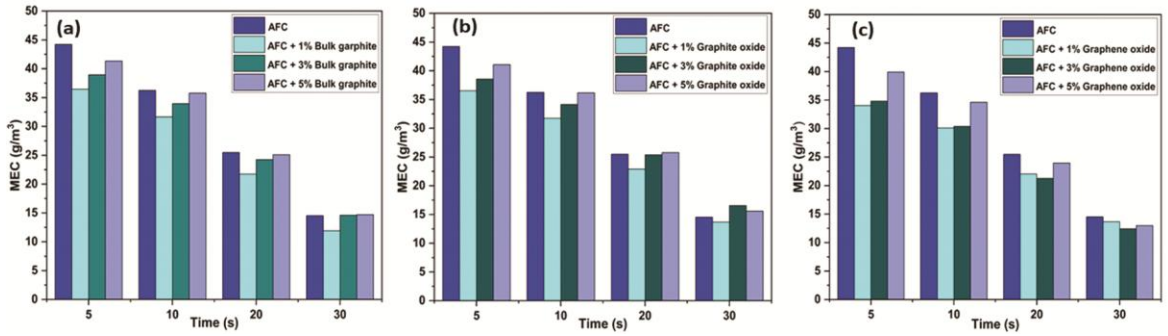

Fig. 10 — MEC of AFCs with (a) bulk graphite, (b) graphite oxide and (c) graphene oxide (1, 3 & 5 %)

MEC was recorded at four different fire extinguishment times (5, 10, 20 & 30 s) considering the literature[21, 39-41] Meenakshi et al. considered the fire extinguishment as positive, when the fire extinguished within 5 sec, however Yan et al. considered 10 sec and UL-2775:2020 & ISO-15779:2011 considered 30 s for class B fire. AFC with graphene oxide showed the least value of MEC (34.03 g/m^3), i.e., the requirement of lesser amount of AFC to extinguish a particular fire (Fig 10). On increasing the percentage of catalysts, MEC increased (39.90 g/m^3), but still it was lesser than that of base AFC. The obtained MEC value of 34.03 g m^{-3} aligns closely with the values reported in the literature, falling within the range of 34-66 g m^{-3} for the incorporation of modifiers[42-43]. Overall, AFC with graphene oxide indicated higher burn rates, lower MECs and comparable values of combustion efficiency. Enhancement in performance of AFC may be due to the high thermal conductivity of added graphene oxide with few graphitic layers[44].

To comprehend the mechanism underlying the catalytic activity of graphene catalyst, AFC burn rate strand was considered as a series of thin layers/disc. The layer which is ignited first is the reacting layer [27]. On its ignition, heat/energy is produced which is transferred to the next layer (pre-reacting layer). The combustion of pre-reacting layer takes place only when energy transferred is greater than the activation energy. Thereafter, when second layer is burnt, it again transfers the energy to next un-reacting layer. This process repeats and sustained burning takes place. Lower the activation energy, lower will be the time required for transfer of energy and burn rate decreases.

Bulk graphite, graphite oxide and graphene oxide, all have good thermal conductivity. Catalysts with good thermal conductivity fasten the transfer of heat between different layers of the AFC strand. This is in turn increases the burn rate of AFC. The thermal conductivity of these graphitic catalysts depends on the number of graphitic layers. When we move from bulk graphite to graphene oxide, the number of graphitic layers decreases. Since graphene oxide has single or few layers as compared to other two, it has highest thermal conductivity. Hence, highest burn rate and lowest combustion temperature (DSC curve in Fig 8) is observed in case of AFC with graphene oxide as a catalyst.

Higher burn rates of AFCs lead to decrease in the granularity of the solid particulates of aerosols and they remain active in air for longer time. In addition, when burn rate is fast, aerosol fills the fire zone in less time and this in turn decreases the fire extinguishing time. Hence, high thermal conductivity of graphene oxide led to enhancement in the ultimate performance of AFC.

Combustion product analysis

For preliminary characterization of solid particulates of aerosols anion group test analysis was done. For nitrate and nitrite group analysis, conc. sulphuric acid was added to collected solid particulates of aerosol. Freshly prepared iron sulphate was added from the side wall to above solution. Firstly, a slight brown ring was formed which disappeared immediately, and solution turned brown in colour which indicated the presence of nitrite/nitrate group. For detecting the presence of bicarbonate and carbonate anion, dilute HCl was added to collected solid particulates of aerosol. Effervescences was produced which was passed to lime water. Lime water turned milky which confirmed the presence of bicarbonate/carbonate[45].

Pyrotechnically generated aerosol particles generally consist of carbonates, bicarbonates, nitrites of potassium and some unsaturated hydrocarbons. To ascertain the chemical structure and composition of

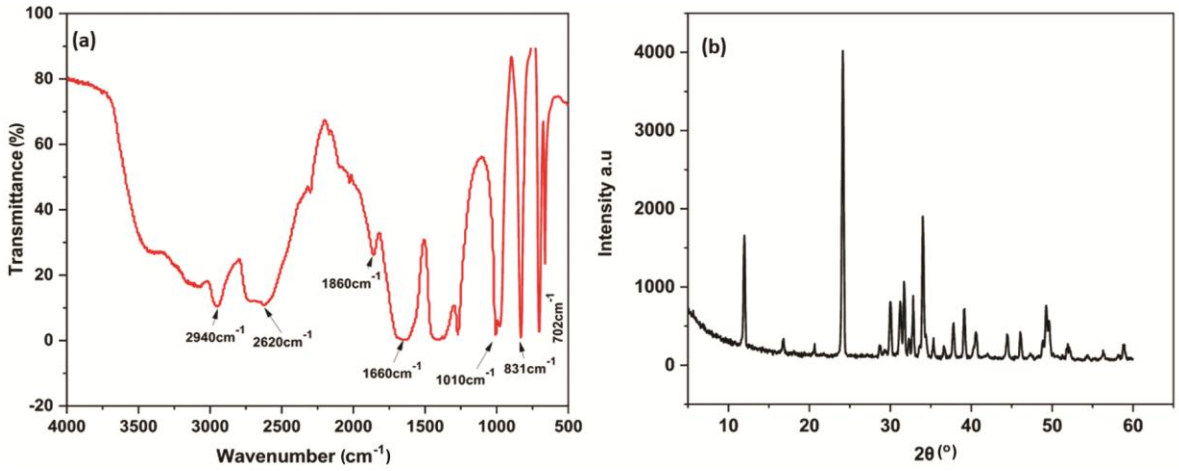

Fig. 11 — Characterization of solid aerosol particles using (a) FTIR and (b) XRD pattern

collected aerosol particles, FTIR and XRD analysis was performed. Peak at 1660 cm^{-1} corresponded to C=O stretching of potassium bicarbonate[46] as shown in Fig 11a. The presence of potassium nitrite and nitrate were also observed around 831 cm^{-1} for N=O stretching[46]. Peaks around 702 and 1010 cm^{-1} corresponded to C-O stretching of potassium carbonate[47]. Unsaturated hydrocarbon peaks were also observed at 2620 and, 2940 cm^{-1} for C-H stretching vibrations[48].

XRD patterns of collected aerosols indicated peaks at 11.98°, 29.98°, 37.17°, 37.82° and 49.38° corresponding to potassium carbonate, Fig 11b. Potassium nitrite/nitrate peaks were obtained at 24.14°, 32.82°, 34.06°, 40.62°, 44.42° and 46.10° (Ref.49). Aerosols The particle size range of the aerosols were calculated using particle counter and found to be in range of 1-2 1-2 µm.

Conclusion

Aerosol forming composites (AFCs) with and without graphite, graphite oxide and graphene oxide (1-5%) were prepared and characterized for combustion efficiency, burn rate, minimum fire extinguishing concentration and mechanical strength. Addition of graphene oxide among other catalysts improved the thermo-kinetic performance of AFC. Combustion temperature reduced from 455 to 409℃ on addition of 5% graphene oxide. Combustion efficiency increased from 77 to 80% on addition of 1% graphene oxide, but further increase to 5% decreased the combustion efficiency to 76%. Increase in burn rate was observed from 9.46 mm/s to 11.78 mm/s (with 5% graphene oxide). MEC decreased from 44.23 to 41.31 g/m^3 with 1% graphene oxide, and it further increased to 42.21 g/m^3 with 5% graphene oxide. Therefore, AFC with 1% graphene oxide clearly indicated finest performance among prepared samples. Such high burn rate AFC with lower MEC values appeared as potential candidate for use with CAFES for fast extinguishment of fires. Collected aerosol particles were found as carbonates, bicarbonates, and nitrites of potassium. Researchers in the same field will find the current study to be helpful when considering using graphene oxide as a highly promising catalyst in aerosol-forming composites.

Acknowledgement

Authors thank Sh. Rajiv Narang, Director, Centre for Fire, Explosives, and Environment Safety, DRDO, Delhi, for his keen interest in the work and providing logistic support. Authors thank Sh. R K Tanwar and Dr. P K Roy for their useful suggestions. Authors also thank SSPL, DRDO for their support in instrumental facility. Authors would also like to thank to competent authority, Guru Gobind Singh Indraprastha University for characterization through FRGS.

References

1 Zhang X, Ismail M H S, Ahmadun F R, Abdullah N H & Hee C, Hot aerosol fire extinguishing agents and the associated technologies: A review, *Braz J Chem Eng*, 32 (2015) 707.

2 Jiang H, Bi M, Huang L, Zhou Y & Gao W, Suppression mechanism of ultrafine water mist containing phosphorus compounds in methane/coal dust explosions, *Energy*, 239 (2022) 121987.

3 Zhang C, Li H, Guo X, Li S, Zhang H, Pan X & Hua M, Experimental and theoretical studies on the effect of $Al(OH)_3$ on the fire-extinguishing performance of superfine ABC dry powder, *Powder Technol*, 393 (2021) 280.

4 Lei B, He B, Xiao B, Du P & Wu B, Comparative study of single inert gas in confined space inhibiting open flame coal combustion, *Fuel*, 265 (2020) 116976.

5 Ge L, Shao Y, Wang Y, Zhang G, Zhang Z & Liu L, Experimental research on inerting characteristics of carbon dioxide used for fire extinguishment in a large sealed space, *Process Saf Environ Prot*, 142 (2020) 174.

6 Wang T, Hu Y, Zhang P & Pan R, Study on thermal decomposition properties and its decomposition mechanism of pentafluoroethane (HFC-125) fire extinguishing agent, *J Fluor Chem*, 190 (2016) 48.

7 Rohilla M, Saxena A, Dixit P K, Mishra G K & Narang R, Aerosol forming compositions for firefighting applications: A review, *Fire Technol*, 55 (2019) 2515.

8 Conkling J & Mocella C, Chemistry of pyrotechnics: basic principles and theory, 2nd Edn, Marcel Dekker, INC, New York, ISBN: 13 (2013) 978.

9 Agafonov V V, Kopylov S S, Sychev A V, Uglov V A & Zhyganov D B, The mechanism of fire suppression by condensed aerosols, Halon Opt. Tech. Work. Conf. Proc 15th, Albuquerque, (2005) 1-10.

10 Rohilla M, Saxena A, Tyagi Y K, Singh I P, Tanwar R K & Narang R, Condensed aerosol based fire extinguishing system covering versatile applications, *Rev Fire Technol*, 58 (2021) 327.

11 Raccichini R, Varzi A, Passerini S & Scrosati B, The role of graphene for electrochemical energy storage, *Nat Mater*, 14 (2014) 271.

12 Yang Q D, Li J, Cheng Y, Li H W, Guan Z, Yu B & Tsang S W, Graphene oxide as an efficient hole-transporting material for high-performance perovskite solar cells with enhanced stability, *J Mater Chem*, 5 (2017) 9852.

13 Yu I K M, Xiong X, Tsang D C, Ng Y H, Clark J, Fan J & Ok Y S, Graphite Oxide- and Graphene Oxide-supported catalysts for microwave-assisted glucose isomerisation in water, *Green Chem*, 21 (2019) 4341.

14 Wei Z, Wang D, Kim S, Kim S Y, Hu Y, Yakes M K & Riedo E, Nanoscale tunable reduction of graphene oxide for graphene electronics, *Science*, 328 (2010) 1373.

15 Liu K K, Jiang Q, Tadepalli S, Raliya R, Biswas P, Naik R R & Singamaneni S, Wood-graphene oxide composite for highly efficient solar steam generation and desalination, *ACS Appl Mater Interf*, 9 (2017) 7675.

16 Krishnan D, Kim F, Luo J, Cruz-Silva R, Cote L J, Jang H D & Huang J, Energetic graphene oxide: Challenges and opportunities, *Nano Today*, 7 (2012) 137.

17 Li R, Wan J, She J P, Hua C & Yang G C, Preparation and characterization of insensitive HMX/graphene oxide composites, *Propellants Explos Pyrotech*, 38 (2013) 798.

18 Yan N, Qin L, Li J, Zhao F & Feng H, Deposition of iron oxide on reduced graphene oxide and its catalytic activity in the thermal decomposition of ammonium perchlorate, *Appl Surface Sci*, 451 (2018) 155.

19 An T, Zhao F Q, Yan Q L, Yang Y J, Luo Y J, Yi J H & Hong W L, Preparation and evaluation of effective combustion catalysts based on Cu(I)/Pb(II) or Cu(II)/Bi(II) nanocomposites carried by graphene oxide (GO), *Propellants Explos Pyrotech*, 43 (2018) 1087.

20 Zhang W, Luo Q, Duan X, Zhou Y & Pei C, Nitrated graphene oxide and its catalytic activity in thermal decomposition of ammonium perchlorate, *Mater Res Bullet*, 50 (2014) 73.

21 Rohilla M, Saxena A & Tyagi Y K, Role of metal oxides on the performance of aerosol forming composites for fire extinguishing application, *J Therm Anal Calorim*, 147 (2022) 8095.

22 Rohilla M, Saxena A & Tyagi Y K, Facile synthesis of rGO/Fe_2O_3 nanocomposite and its combination with aerosol forming composite for ultra-fast fire extinguishment, *J Mater Sci*, 58 (2023) 1640.

23 Yan Y, Du Z & Han Z, A novel hot aerosol extin-guishing agent with high efficiency for Class B fires, *Fire Mater*, 43 (2018) 84.

24 Marcano D C, Kosynkin D V, Berlinx D V, Sinitskii A, Sun Z, Slesarev A & Tour J M, Improved Synthesis of Graphene Oxide, *ACS Nano*, 4 (2010) 4806.

25 Zaaba N I, Foo K L, Hashim U, Tan S J, Liu W W & Voon C H, Synthesis of graphene oxide using modified hummers method: Solvent influence. *Procedia Eng*, 184 (2017) 469.

26 Zhang K K, Suh J M, Lee T H, Cha J H, Choi J W, Jang H W & Shokouhimehr M, Copper oxide-graphene oxide nanocomposite: Efficient catalyst for hydrogenation of nitroaromatics in water, *Nano Converg*, 6 (2019) 1.

27 Sanoop P S, Rajeev R R & Georgea B K, Graphite oxide–iron oxide nanocomposites as a new class of catalyst for the thermal decomposition of ammonium perchlorate, *RSC Adv*, 6 (2016) 45977.

28 Zhang M, Zhao F, Yang Y, Zhang J, Li N & Gao H, Effect of rGO–Fe_2O_3 nanocomposites fabricated in different solvents on the thermal decomposition properties of ammonium perchlorate, *Cryst Eng Comm*, 20 (2018) 7010.

29 Rohilla M, Saxena A & Tyagi Y K, Factors affecting the burn rate and combustion temperature of fire-extinguishing aerosol-forming composite material, *J Mater Res*, 38 (2023) 789.

30 Udupa M R, Thermal decomposition of potassium nitrate in the presence of chromium(III) oxide, *Thermochim Acta*, 6 (1976) 231.

31 Pei J, Zhao H, Yang F & Yan D, Graphene Oxide/Fe2O3 Nanocomposite as an efficient catalyst for thermal decomposition of ammonium perchlorate via the vacuum-freeze-drying method, *Langmuir*, 37 (2021) 6132.

32 Kozyrev V N, Yemelyanov V N & Andreev V A, Aerosol forming composition for the purpose of extinguishing fires, *Patent US*, (1998) 5831209.

33 Drakin N V, Pyrotechnical aerosol forming composition for extinguishing fires and processes for its preparation, *Patent US*, B1 (2001) 6264772.

34 Kozyrev V K, Yemelyanov V N, Sidorov A I & Andrrev V A, Aerosol forming composition for the purpose of extinguishing fires and methods for the preparation of this composition, *Patent US*, (2000) 6042664.

35 Drakin N V, Method and apparatus for extinguishing fires, *Patent US*, (2000) 6089326.

36 Zhang Y, Liao G, Pan R & Wang H, The influencing factors of HEAE burning rate and fire suppression efficiency, *J Chem Health Saf*, 13 (2005) 13.

37 Yonghua H, Steam hot aerosol fire extinguishing composition and its use method and fire extinguishing device, *Patent CN*, (2011) 101554520.

38 Rusin D, Denisyuk A, Michalev D & Shepelev J, Pyrotechnical aerosol-forming fire-extinguishing composite and a method of its production, *Patent US*, B2 (2004) 6689285

39 Kosanke B J & Kosanke K L, Control of pyrotechnic burn rate, *J Pyrotecnics Archive*, 3 (1994) 265.

40 Yan Y, Du Z & Han Z, A novel hot aerosol extinguishing agent with high efficiency for Class B fires, *Fire Mater*, 43 (2019) 84.
41 Standard for fixed condensed aerosol extinguishing system units, (2019) UL2775.
42 Denisyuk A, Pyrotechnical aerosol forming fire extinguishing composite and a method of its production, *Patent EU*, A2 (2003) 134158.
43 Zeliff Z, Loveless L & Kutsel V & Doronichev, Low temperature flameless aerosol producing fire extinguishing composition and production method thereof, *Patent US*, A1 (2010) 20100294975.
44 Balandin A A, Ghosh S, Bao W, Calizo I, Teweldebrhan D, Miao F & Lau C N, Superior Thermal Conductivity of Single-Layer Graphene, *Nanotechnol Lett*, 8 (2008) 902.
45 Pandey O P, Bajpayee D N & Giri S S, *Practicle Chemistry Book*, ISBN-10: 8121908124, (1972).
46 Miller A F & Wilkins C H, Infrared spectra and characteristic frequencies of inorganic ions, *Anal Chem*, 24 (1952) 1253.
47 Han S J & Wee J H, Carbon dioxide capture and carbonate synthesis via carbonation of KOH dissolved alcohol solution, *J Korean Soc Environ Eng*, 37 (2015) 597.
48 Lin S K, Mai Y J, Li S R, Shu C W & Wang C H, Characterization, and hydrogen storage of surface-modified multiwalled carbon nanotubes for fuel cell application, *J Nanomater*, 2012 (2012) 1.
49 Rohilla M, Saxena A, Prakash B, Tanwar R K, Narang R & Tyagi Y K, Hematite particle size effect on combustion performance of fire extinguishing composites, *Chemistry Select*, 8 (2022) e202204542.